Proceedings of the 3rd International Congress APMAS2013, April 24–28, 2013, Antalya, Turkey

Influence on Static Grain Growth and Sinterability of BaO Addition into 8YSZ

B. Aktas[a,*], S. Tekeli[b] and S. Salman[c]

[a]Harran University, Engineering Faculty, Department of Mechanical Engineering, 63300, Sanliurfa, Turkey
[b]Gazi University, Technology Faculty, Metallurgical and Materials Engineering Department, 06500, Ankara, Turkey
[c]Mehmet Akif Ersoy University, Faculty of Engineering and Architecture, Burdur, Turkey

In this study, 8 mol.% yttria stabilized cubic zirconia (8YSZ) powders as a matrix material and 0–15 wt% BaO powders as an additive were used in order to determine the effect of BaO addition and amount on the microstructure, sintering and static grain growth properties of the 8YSZ. For these purposes, undoped and BaO-doped 8YSZ specimens were annealed for grain growth at 1400, 1500, and 1600 °C for 10, 50, and 100 h, respectively. An increase of annealing temperature and holding time resulted in grain growth in all specimens. The grain size of the 8YSZ decreased with the higher level of BaO added. A limited amount of BaO dissolved in 8YSZ, and insoluble BaO reacted with ZrO_2 at high sintering temperature and generated the $BaZrO_3$ second sphase compound. Energy dispersive X-ray spectroscopy results showed that the $BaZrO_3$ second phase segregated at the surrounding grains and grain boundaries of the 8YSZ. These $BaZrO_3$ second phases had a pinning effect at the grain boundaries and prevented the migration of the grain boundaries of the 8YSZ. In conclusion, the grain growth results showed that the grain growth in the BaO-doped 8YSZ specimens was controlled by a solid solution drag mechanism.

DOI: 10.12693/APhysPolA.125.652
PACS: 81.05.Je, 81.07.Bc, 81.20.Ev

1. Introduction

Grain growth is the process by which the average grain size of the material increases continuously during heat treatment without a change in grain size distribution [1]. Theoretically, given a high enough temperature, in the absence of a driving force such as a secondary phase, a polycrystalline solid will grow to single crystal, but in reality this goal is never achieved [2]. The importance of controlling grain growth in ceramics is twofold: materials properties vary with grain size and it may be necessary to prepare articles of close-to-theoretical density [3]. Grain growth takes place in three stages: primary recrystallization, grain growth, and secondary recrystallization. Primary recrystallization is a process by which the nucleation and growth of a new generation of grains occur either in an amorphous material or in a matrix which has been previously deformed plastically [1]. Various parameters affect the grain size of ceramic materials: sintering temperature, sintering time, the availability of porosity, and the second phase in the microstructure.

Solid oxide fuel cells (SOFCs) are used in the various applications, such as energy production and in the automotive and aerospace industries [4]. Fuel cells typically have a pair of electrodes (anode and cathode) and an electrolyte. The working principle of a fuel cell is similar to that of a battery. However, unlike a battery, a fuel cell does not run down or require recharging. A fuel cell operates as long as both fuel and oxidant are supplied to electrodes [5]. Yttria-stabilized cubic zirconia (8YSZ) with a fluorite structure is known as a solid electrolyte. Due to the high oxygen ion conductivity, the fact that it remains chemically stable at high temperatures and its features such as partial oxygen pressure, 8YSZ is widely used as SOFC, oxygen sensor and thermal barrier [6]. In these applications, not only high conductivity, but also better mechanical, chemical and electrical stability, is required [7].

ue to the need for a high operating temperature (1000 °C) in the SOFCs, a lower operating efficiency occurs at high operating temperatures [8]. In addition, the mechanical strength of 8YSZ also decreases with holding at high temperatures for a long time. This situation restricts the use of the material as a solid electrolyte. Due to the resulting heat stresses, the mechanical stresses during the process, and excessive grain growth, the 8YSZ that is used in these conditions breaks easily [9]. For these reasons, the improvement of the mechanical properties of 8YSZ used as a solid electrolyte is an important problem to be solved. 8YSZ exhibits the low mechanical strength, due to the occurence of grain growth under high operating temperature in SOFCs. Therefore, in this study, the grain growth kinetics and sinterability of BaO-doped 8 mol.% yttria-stabilized cubic zirconia was investigated (8YSZ).

2. Experimental materials and procedure

In this study, 8YSZ powders (Tosoh, Japan) and BaO powders (Taimei, Japan) up to 15 wt% were used as matrix material and additive, respectively. The average grain sizes were 0.3 μm for 8YSZ and 0.4 μm for BaO. The chemical compositions of the powders used in the experiments are presented in Table.

The specimens for the microstructural investigations were produced by means of colloidal processing. The doping process was carried out in a plastic container by

*corresponding author; e-mail: baktas@harran.edu.tr

TABLE

The chemical composition of powders used in the experimental works (in wt%).

Powder	ZrO_2	Y_2O_3	BaO	TiO_2	FeO_2	Na_2O_3	CaO	Al_2O_3	SiO_2
8YSZ	85.9	13.6	–	0.1	0.003	0.01	0.02	0.25	0.1
BaO	–	–	99.9	–	0.02	–	–	0.01	0.07

the mechanical mixing of BaO up to 15 wt% and 8YSZ powders with zirconia balls and ethanol. The mechanical mixing was done in a "speks" type mixer at 200 rev/min for 12 h. The prepared slurries were left to dry for 24 h by leaving the lid open. After the drying process, the agglomerated powders with medium hardness were ball milled for 10 min to obtain a good dispersion and to break up the agglomerates. The powders obtained were sieved through a 60 μm sift and pressed under a 200 MPa pressure in a single axis die with a radius of 10 mm and a height of 5 mm. The inner surface of the steel die was cleaned after each dry pressing process and stearic acid was applied to the side walls of the die.

Sintering was carried out in a box type furnace under normal atmospheric conditions. The pressed pellets were first subjected to a presintering process at 1000 °C and then sintered at temperatures between 1200 and 1550 °C for 1 h at heating and cooling rates of 5 °C/min. The density of the sintered specimens with perfect shape was calculated by using the rule of mixtures and obtaining the ratio between weight and volume, which was determined by a geometrical method. The relative density was estimated on the assumption that the sintered body was at the cubic phase and was based on the theoretical density of 5.68 and 5.72 g/cm^3 for 8YSZ and BaO, respectively. The grain growth processes of sintered specimens at optimum sintering temperature were carried out by means of annealing at 1400, 1500, and 1600 °C for 10, 50, and 100 h, respectively. The surfaces of the specimens were ground and polished using the normal metallographic methods after the sintering process and the specimens were thermally etched by keeping them in a furnace at 50 °C below the sintering temperature for 1 h. The microstructural investigation of the sintered specimens was performed using a scanning electron microscope (SEM JEOL Lv 6060). Grain sizes were measured using the mean linear intercept method.

3. Experimental results and discussion

The microstructures of the undoped and the different amounts of BaO-doped 8YSZ specimens annealed at 1400 °C for 100 h are presented in Fig. 1. The undoped 8YSZ specimen has an equiaxed, angular and coarse-grained structure, whereas the BaO doped 8YSZ specimens have an equiaxed, uniformly distributed, porous and fine-grained structure. The fine-grained structure found at the grain boundaries of the 8YSZ specimens belongs to the $BaZrO_3$ compound. It was found that this second phase at the grain boundaries of 8YSZ belonged to $BaZrO_3$ compound by XRD and EDS. $BaZrO_3$ secondary phase is formed by the reaction of insoluble BaO in the 8YSZ matrix with ZrO_2 at high temperatures. As can be seen from microstructures, grain growth occured with the elevation of the annealing temperature and dwell time in the undoped and BaO-doped 8YSZ specimens. The grain growth came about at the highest rate in the undoped 8YSZ and occurred at the lowest rate in the 15 wt% BaO-doped 8YSZ specimen.

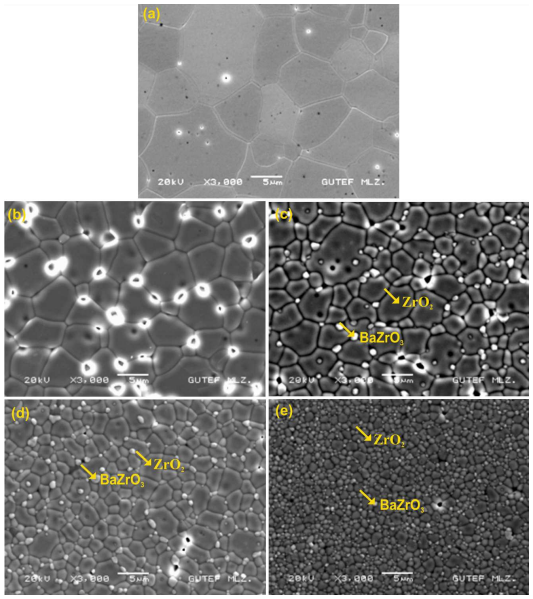

Fig. 1. The microstructures of the undoped and the different amounts of BaO doped 8YSZ specimens annealed at 1400 °C for 100 h. (a) Undoped, (b) 1, (c) 5, (d) 10, and (e) 15 wt% BaO doped 8YSZ.

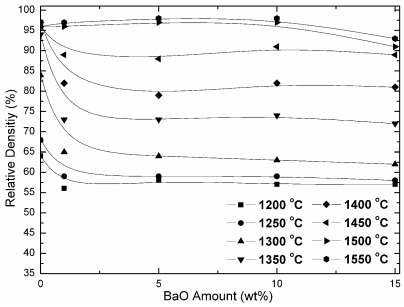

Fig. 2. Relative density of the undoped and the different amounts of the BaO doped 8YSZ specimens sintered at various temperatures for 1 h.

The effect of the BaO addition and dopant amount on the sinterability of the 8YSZ is presented in Fig. 2. For all compositions, the relative density of the specimens increased with elevating sintering temperature. It can also be seen from this figure that the sintered density of the 8YSZ specimens decreased with increasing BaO content. Hence higher sintering temperatures were necessary to densify the specimens. The retardation of densification in the specimens with higher amount of BaO could be due to a number of reasons. Firstly, the microstructural investi-

gations showed that in the specimens with higher amount of BaO, there was a high level of porosity in the grain interior and along the grain boundaries. These porosities hindered the sintered density. Secondly, it is known that the $BaZrO_3$ phase, which is formed by the reaction between 8YSZ and BaO at high temperatures, is very hard to sinter. Finally, the grain boundary diffusion of the 8YSZ could be decreased by the $BaZrO_3$ grains because the 8YSZ grains around the perimeter of the $BaZrO_3$ particles were unable to contact each other freely. The $BaZrO_3$ grains were mostly located at the grain boundaries which caused the grain boundary diffusion bath to be longer and thus the diffusion of atoms along grain boundaries between 8YSZ and $BaZrO_3$ became slower. These results indicated that higher amount of BaO addition inhibited densification by decreasing grain boundary diffusion.

The EDS analysis results of 15 wt% BaO doped 8YSZ sintered at 1500 °C for 100 h are presented in Fig. 3. The EDS analysis results showed that insoluble BaO in the 8YSZ matrix precipitated as a $BaZrO_3$ compound at the grain boundaries and among the grains of 8YSZ. According to EDS results received from the point B, the presence of Ba^{2+}, Zr^{4+} and O^{2-} at the point B showed that the $BaZrO_3$ compound formed at the grain boundaries and along the grains of 8YSZ.

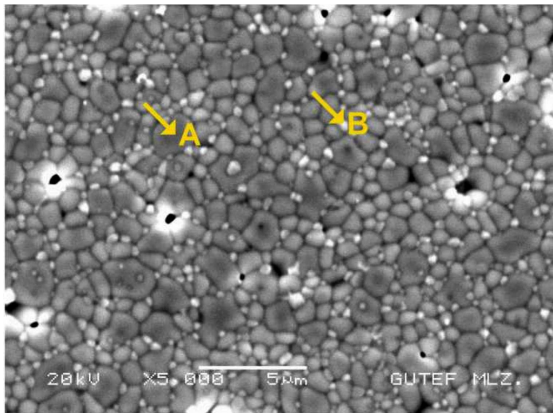

Fig. 3. EDS analysis of 15 wt% BaO doped 8YSZ sintered at 1500 °C for 100 h.

	wt% content			
Point of EDS analysis	Zr^{4+}	Ba^{2+}	Y^{3+}	O^{2-}
A	60.350	8.980	13.029	17.641
B	56.795	12.071	14.969	16.165

The grain sizes of the specimens doped with various amounts of BaO after annealing at 1400 °C for 10, 50, and 100 h are presented in Fig. 4. After annealing, grain coarsening occurred in the undoped 8YSZ. The grain size measurement results showed that the grain size of 8YSZ decreased with increases of the amount of BaO dopant. BaO dopant can be dissolved up to 1 wt% content in the 8YSZ matrix. BaO, which could not be dissolved above 1 wt% amount (5, 10, and 15 wt% BaO) in the 8YSZ, precipitated as $BaZrO_3$ secondary phase at the

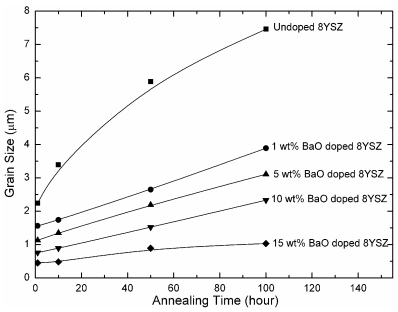

Fig. 4. The grain sizes of the undoped and with various amounts of BaO doped 8YSZ specimens after annealing at 1400 °C for 10, 50, and 100 h.

grain boundaries and along the grains of 8YSZ. The existence of the $BaZrO_3$ compound at the grain boundaries of 8YSZ inhibited the migration of grain boundaries and brought about a decrease in the grain size of 8YSZ.

Due to the low solubility of BaO in the 8YSZ matrix, BaO existed as a secondary phase at the grain boundaries of 8YSZ. This secondary phase acted as a barrier against the diffusion of grain boundaries. When undoped 8YSZ was compared to BaO-doped 8YSZ specimens, it appeared that the cation segregation was limited at the grain boundaries in the undoped 8YSZ and the grain growth came about faster in the undoped 8YSZ. As a result, the grain boundaries of undoped 8YSZ have a lower cohesive strength and higher grain boundary mobility and grain boundary energy. Therefore, the grain growth in the undoped 8YSZ occurred more rapidly. Grain growth kinetics were determined using the following equations:

$$D^n - D_0^n = K(t - t_0), \tag{1}$$

$$K = K_0 \exp(-Q/(RT)), \tag{2}$$

where D is grain size in duration t, D_0 is the initial grain size, n is grain growth exponent, K is a kinetic constant dependent on grain boundary and temperature, K_0 is a constant not dependent on temperature and Q, R, and T are activation energy, gas constant, and the absolute temperature, respectively.

The grain growth exponent (n) is calculated from the slope of the line obtained from the plot of $\log(D)$–$\log(t)$ as shown in Fig. 5. The grain growth exponent (n) values for the undoped and BaO-doped 8YSZ specimens were calculated as 3. In this study, the value of grain growth exponent was 3 in the undoped 8YSZ. This n value for undoped 8YSZ showed that it conformed with the literature [10]. That it was $n = 3$ of the grain growth exponent value in the BaO-doped 8YSZ specimens shows that the $BaZrO_3$ secondary phases precipitated at the grain boundaries of 8YSZ. It also showed that the grain growth of BaO-doped 8YSZ specimens was controlled by solid solution drag mechanism.

The activation energies for the grain growth of the undoped and BaO-doped 8YSZ specimens are presented in Fig. 6. The activation energy results showed that

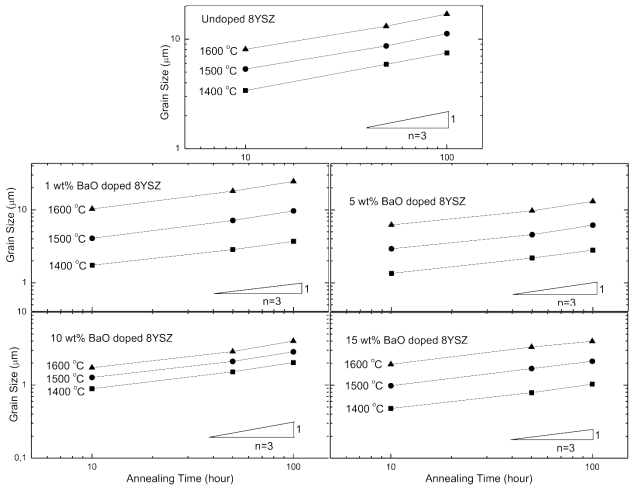

Fig. 5. The grain growth exponent values for the undoped and BaO doped 8YSZ at different temperatures and holding times.

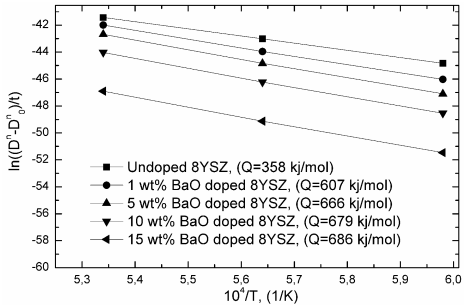

Fig. 6. The grain growth activation energies of undoped and BaO doped 8YSZ specimens.

the activation energies of the BaO-doped 8YSZ specimens were higher than those of undoped 8YSZ. The activation energy for undoped 8YSZ was calculated as 358 kJ/mol, and the activation energies for 1, 5, 10, and 15 wt% BaO-doped 8YSZ specimens were calculated as being approximately 607, 666, 679, and 686 kJ/mol, respectively. The high activation energies in the BaO--doped 8YSZ specimens show that the grain growth level of BaO-doped 8YSZ specimens were lower than that of the undoped 8YSZ. Preventing or reducing grain growth can be achieved by reducing grain boundary mobility and grain boundary energies, through impurities, defects, additives and second phase particles in the material [11].

The grain boundary mobility decreases with increases in the grain boundary width or grain boundary length [12]. In this study, the grain size of 8YSZ decreased with increases in the amount of BaO added. The grain boundary length or total volume of grain boundary increased with BaO addition. BaO, which has low solubility in the 8YSZ matrix, existed as $BaZrO_3$ secondary phase at the grain boundaries of 8YSZ. $BaZrO_3$ secondary phase at the grain boundaries brought about a lowering of the grain boundary diffusion and this phase hindered the grain growth through solid solution drag.

4. Conclusion

EDS analysis and the microstructures of BaO-doped 8YSZ specimens showed that BaO dopant could be dissolved up to 1 wt% content in the 8YSZ and after 1 wt% BaO addition, it precipitated as $BaZrO_3$ second phase at the grain boundaries and around the grains of 8YSZ. The sintering temperature of 8YSZ increased with the addition of BaO and a decrease in the densities of specimens occurred with an increase in the amount of BaO dopant used. The $BaZrO_3$ grains were mostly located at the grain boundaries, which caused the grain boundary diffusion bath to be longer and thus the diffusion of atoms along grain boundaries between 8YSZ and $BaZrO_3$ became slower. These results indicated that the addition of higher amounts of BaO inhibited densification by decreasing the level of grain boundary diffusion.

Due to the low solubility of BaO in the 8YSZ and owing to the existence of $BaZrO_3$ second phase at the grain boundaries, grain growth in the BaO doped 8YSZ specimens occurred at a lesser rate than undoped 8YSZ. The grain growth exponent (n) for undoped and BaO-doped 8YSZ specimens was calculated as $n = 3$. The fact that the value of n was $n = 3$ in the undoped and BaO-doped 8YSZ specimens is due to the segregation of the second phases at the grain boundaries. It also showed that the grain growth was controlled by solid solution drag mechanism of second phases at the grain boundaries. The activation energy results showed that the activation energies of BaO-doped 8YSZ specimens were higher than those of undoped 8YSZ. The high activation energies in the BaO-doped 8YSZ specimens showed that the grain growth of BaO-doped 8YSZ specimens would be lower than undoped 8YSZ.

Acknowledgments

The authors thank Gazi University and Marmara University, Turkey, for the provision of laboratory facilities.

References

[1] W.D. Kingery, H.K. Bowen, D.R. Uhlmann, *Introduction to Ceramics*, 2nd ed., Wiley, New York 1976.

[2] H.V. Atkinson, *Acta Metall.* **36**, 469 (1988).

[3] R.J. Brook, in: *Treatise on Materials Science and Technology*, Ed. F.F. Wang, Academic Press, New York 1976, p. 331.

[4] M.M. Bucko, *J. Europ. Ceram. Soc.* **24**, 1305 (2004).

[5] N.P. Bansal, D. Zhu, *Ceram. Int.* **31**, 911 (2005).

[6] N. Bamba, Y.H. Choa, T. Sekino, K. Niihara, *J. Europ. Ceram. Soc.* **18**, 693 (1998).

[7] S.P.S. Badwal, *Solid State Ionics* **52**, 23 (1992).

[8] T. Zhang, Z. Zeng, H. Huang, P. Hing, J. Kilner, *Mater. Lett.* **57**, 124 (2002).

[9] S. Tekeli, U. Demir, *Ceram. Int.* **31**, 973 (2005).

[10] A.A. Sharif, P.H. Imamura, T.E. Mitchell, M.L. Mecartney, *Acta Mater.* **46**, 3863 (1998).

[11] L.A. Xue, I.W. Chen, *J. Am. Ceram. Soc.* **73**, 3518 (2002).

[12] S. Tekeli, M. Erdogan, B. Aktas, *Mater. Sci. Eng. A* **386**, 1 (2004).